Engineering Fracture Mechanics, vol. 72, 2005, 877-897

The determination of the mode II adhesive fracture resistance, G_{IIC}, of structural adhesive joints: An effective crack length approach.

B.R.K. Blackman[*], A.J. Kinloch[*] & M. Paraschi

Department of Mechanical Engineering, Imperial College London,
Exhibition Road, London SW7 2BX. UK.

Abstract

This paper reports results from the mode II testing of adhesively-bonded carbon-fibre reinforced composite substrates using the end-loaded split (ELS) method. Two toughened, structural epoxy adhesives were employed (a general purpose grade epoxy-paste adhesive, and an aerospace grade epoxy-film adhesive). Linear Elastic Fracture Mechanics was employed to determine values of the mode II adhesive fracture energy, G_{IIC} for the joints via various forms of corrected beam theory. The concept of an effective crack length is invoked and this is then used to calculate values of G_{IIC}. The corrected beam theory analyses worked consistently for the joints bonded with the epoxy-paste adhesive, but discrepancies were encountered when analysing the results of joints bonded with the epoxy-film adhesive. During these experiments, a micro-cracked region ahead of the main crack was observed, which led to difficulties in defining the *true* crack length. The effective crack length approach provides an insight into the likely errors encountered when attempting to measure mode II crack growth experimentally.

Keywords: Adhesive joints; Mode II; Fracture mechanics; Corrected beam theory; End-loaded split test; Microcracking; Effective crack length

---

*Corresponding authors: Tel. +44-20-7594-7196; fax +44-20-7594-7017; email address: b.blackman@imperial.ac.uk (B.R.K. Blackman), Tel. +44-20-7594-7082; fax +44-20-7594-7017; email address: a.kinloch@imperial.ac.uk (A.J. Kinloch)

List of symbols and abbreviations

a	Measured crack length
a_c	Calculated crack length
a_e	Effective crack length
b	Width of joint
C	Compliance (C=δ/P)
C_o	Uncracked beam compliance (with a=0)
CBT	Corrected beam theory
CBTE	Corrected beam theory with effective crack length
δ	Displacement
Δ_I	Mode I length correction
Δ_{II}	Mode II length correction
Δ_{clamp}	Clamp correction
E_1	Flexural modulus of substrate
ECM	Experimental compliance method
ELS	The end-loaded split test
F	Finite displacement correction factor
G_{IC}	Mode I adhesive fracture energy
G_{IIC}	Mode II adhesive fracture energy
h	Height of substrate beam
L	Free length (between the clamp point and the load line) in the ELS test
l_1	Height of loading pin above upper substrate neutral axis
l_2	Half loading block length
m	Slope to the C versus a^3 data
N	Correction factor to account for the loading block.
P	Load
θ	See Appendix
SBT	Simple beam theory

1. Introduction

Previous research has focussed on the development of test methods and data analysis schemes for the determination of mode I adhesive fracture energies in structural adhesive joints. Following a multi-laboratory round-robin exercise [1], this work led to the publication of a new British Standard [2] for the determination of G_{IC}. However, the mode II, or in-plane shear, loading mode has particular importance for adhesive joints and fibre-reinforced composites because cracks will frequently be directionally constrained by the nearby substrates, or layers of fibres in a composite, to grow parallel to this constraint. In addition, adhesive joints are usually designed to minimise any applied mode I loading (to which the joints have least fracture resistance) in favour of designs which promote mode II loading (to which they have greater crack resistance) [3].

Mode II loading may be induced when a cracked adhesive joint or composite is subjected to bending and the various experimental fracture mechanics approaches to mode II usually utilize some form of test specimen which is subjected to applied bending loads with a view to determining values of the critical energy release rate for fracture, G_{IIC}. Some popular mode II adhesive joint test specimens are shown in Figure 1, some having been adapted from earlier work on fibre reinforced polymer composites. Such specimens utilise a thin bondline (shown magnified for clarity in Figure 1) and contain a non-adhesive insert film extending from one end of the joint, in the centre of the adhesive layer, to act as a crack starter.

Figure 1(a) shows the end-notched flexure (ENF) test specimen which is loaded in 3-point bending as shown to induce crack initiation. The test is however, intrinsically unstable and thus may only be used readily to obtain initiation values of G_{IIC}. The four-point bend variant of this test as shown in Figure 1(b) has been proposed more recently [4] and has the advantage that stable crack growth can be achieved. Also, stable crack growth may be obtained from the end-loaded split (ELS) test as shown in Figure 1(c), where the beam is clamped rigidly in the vertical direction whilst being able to slide freely in the horizontal direction. Both the 4-point ENF and the ELS tests allow the full resistance curve (R-curve) to be deduced for the composite or adhesive joint and the choice of which to use will depend upon the availability of apparatus, and the important requirement that the deformation of the substrate beams remain elastic during the test. For relatively tough material systems this requirement favours the ELS over the 4-ENF test method.

The 4-ENF and the ELS test methods require that the load, load-point displacement and crack length be determined at crack initiation and during any subsequent stable crack propagation. Whilst the measurement of the load and displacement can usually be achieved to high accuracy, the measurement of the crack length as the crack propagates under mode II loading is not a trivial matter, as will be discussed later. It is noteworthy, that the use of height contoured beams as shown in Figure 1(d) [5, 6] is becoming more popular for mode II testing, as this may eliminate the need to measure the length of the propagating crack. However, these joint designs are more complicated and expensive to manufacture. Also, for fibre composite substrates when flat sheets are firstly prepared, this type of specimen requires backing beams to be employed to provide the contour.

One of the main problems that has been encountered when loading in mode II has been the poor reproducibility of values of the measured G_{IIC}. [7]. The effects of friction in the test, the complex damage mechanisms occurring at the crack tip and the lack of a universally agreed test standard have all been suggested as the primary cause of this problem of poor reproducibility.

Various workers have considered the effects of friction in mode II composite delamination tests. Carlsson et al [8] performed an analysis of the ENF specimen and concluded that, for composites, an error of between 2-4% would be encountered in the measured values of G_{IIC} by neglecting friction. Experimental load-unload cycles performed by Russell and Street [9] implied a maximum error of around 2% in G_{IIC} in composites if friction was ignored. The effects of friction during mode II ENF and ELS tests on adhesive joints was assessed experimentally by Fernlund and Spelt using a modified test fixture that eliminated surface tractions in the wake of the crack [10]. They concluded that whilst friction effects did exist in these tests, they were relatively small. More recently, Schuecker and Davidson, [11, 12] considered the effects of friction in the ENF and 4-ENF tests on composites and concluded that friction accounted for about 2% and 5% respectively of the measured values of G_{IIC} from these tests. However, these authors also concluded that other effects, such as crack length measurement, were also important factors in the accuracy of mode II tests. Davies [13] showed experimentally that frictional effects could account for up to 20% of the measured G_{IIC} values in the ENF test if PTFE spacers were not used. Finally, Blackman and Williams [14] considered friction effects in the ELS test by including a frictional shear stress in the beam analysis. Although friction effects were shown to be significant for the composites studied, their results were dependent upon the accuracy of both the corrected beam theory and experimental compliance data analysis methods. These methods, as shown later in the present work, are sensitive to errors in measured crack length so it is important to take account of these effects first.

Some recent work [15-17] has indicated that a major cause of scatter and inconsistency in mode II data analyses may be a difficulty in defining the location of the crack tip. The difficulty in defining the true crack length has also been observed during G_{IC} tests in composites when extensive fibre-bridging and micro-cracking occurs. This has been shown to lead to variations and errors in the data analysis when corrected beam theory is employed [16, 17]. These variations are most readily identified via the incorrect values of flexural modulus that are back-calculated from the mode I analysis, and also from the large scatter in the values of the beam theory root rotation correction, Δ, so deduced.

In the present work the various length corrections to beam theory are discussed, and an improvement to the free length correction in the ELS test is proposed to account for the clamping condition. Also, a calibration procedure is described in which the values of crack length are deduced from corrected beam theory and experimental compliance, and these are then used to calculate values of G_{IIC}. Such a procedure has provided an insight into the likely errors encountered when attempting to measure crack length experimentally during mode II loading.

2. Analysis

2.1 Simple Beam Theory

The compliance, C, of the ELS specimen shown in Figure 2 may be expressed as [18]:

$$C = \frac{\delta}{P} = \frac{3a^3 + L^3}{2bh^3 E_1} \tag{1}$$

where P is the applied load, δ, the load-line displacement and the lengths a, L and h are as defined in Figure 2. The substrate beams have a width, b, and a known flexural modulus E_1. This analysis was developed for unidirectional fibre-reinforced polymer composites but is applicable to adhesive joints with relatively thin bond-lines provided that the flexural modulus of the substrate is much greater than the Young's modulus of the adhesive. Equation (1) may be differentiated with respect to the crack length, *a*, and substituted into the Irwin-Kies equation (2):

$$G_{IIC} = \frac{P^2}{2b} \cdot \frac{dC}{da} \tag{2}$$

to yield an expression for the adhesive fracture energy in mode II, G_{IIC} [18]:

$$G_{IIC} = \frac{9P^2a^2}{4b^2h^3E_1} \tag{3}$$

2.2 Corrected Beam Theory Analyses

2.2.1 Corrected beam theory with assumed length corrections

Equation (1) can be corrected for the effects of transverse shear and beam root rotation at the crack tip and clamping point via the addition of correction factors to the crack length, *a* and the clamp length, *L*. In the original work on fibre-composites by Hashemi et al [18], the same length correction, Δ, was applied to both *a* and *L* and the value of the correction was determined from a mode I DCB test. These authors did however, optimise the value of the correction term used by fitting the calculated values of compliance from the ELS test to the experimental data. In a subsequent numerical study [19], different length corrections were applied to *a* and *L* to correct the compliance as shown in equation (4), where *N* is an additional correction factor to account for the effects of applying the load to the specimen via a bonded-on end block (see Appendix 1):

$$C = \frac{\delta}{P} = \frac{3(a + \Delta_{II})^3 + (L + 2\Delta_I)^3}{2bh^3E_1} \cdot N \tag{4}$$

It was suggested that the crack length, *a*, should be corrected by the value Δ_{II} and the free length *L* should be corrected by $2\Delta_I$. The correction on *L* was $2\Delta_I$ because the clamping at *L* was described as being analogous to the clamping assumed at the crack tip in the mode I DCB test, where Δ_I was used to correct the length, but now with the modification that the entire beam was flexed in the same sense (hence $2\Delta_I$). These authors found that by using a finite element calibration procedure [19] Δ_{II} could be obtained directly from the Δ_I value and:

$$\Delta_{II} = 0.42\Delta_I \tag{5}$$

was appropriate for a mode II test where Δ_I is the value of the mode I correction measured in a DCB test. The corrected expression for G_{IIC} was thus:

$$G_{IIC} = \frac{9P^2(a + \Delta_{II})^2}{4b^2h^3E_1} \cdot F \tag{6}$$

where F is a correction factor to account for large deflections (see Appendix 1) and this version of analysis was adopted in the ESIS TC4 test protocol for fibre-composites [20].

2.2.2 Corrected beam theory with experimentally determined clamp correction

The above procedure for determining both length corrections from mode I DCB test data has a number of disadvantages. Firstly, the assumption that the constraint at the clamping point can be assumed to be equivalent to the notional constraint at the crack tip in a DCB test may not be valid. Indeed, it is shown in the present work that this correction procedure would lead to an over-correction of L. Secondly, such a correction should take into account the severity of the clamping used in the ELS test, i.e. a lightly clamped specimen would deflect and rotate more at the clamp point than a tightly clamped specimen. Basing this correction on the mode I value does not allow the clamping torque to be taken into account. Finally, it is known that the mode I correction procedure, which fits the measured experimental mode I data for an individual test, produces values of Δ_I which vary quite significantly from test to test, as was discussed by Brunner et al [16]. To use a mode I value obtained in a separate test to derive a mode II value obviously requires some average value to be used, thus the correction for any individual test may be in error.

In the present work, the length correction to L was also determined experimentally using an 'inverse ELS test' as will be described in Section 3. This correction is referred to here as Δ_{clamp}. Thus, the compliance of the joint can be written as:

$$C = \frac{\delta}{P} = \frac{3(a + \Delta_{II})^3 + (L + \Delta_{clamp})^3}{2bh^3 E_1} \cdot N \tag{7}$$

and in the 'inverse ELS test' the cracked portion of the joint is held fully within the clamp, so that a=0, (and thus Δ_{II} does not apply) and the un-cracked beam compliance, C_o, is then given by:

$$\left(\frac{C_o}{N}\right)^{\frac{1}{3}} = \left(\frac{1}{2bh^3 E_1}\right)^{\frac{1}{3}} L + \left(\frac{1}{2bh^3 E_1}\right)^{\frac{1}{3}} \Delta_{clamp} \tag{8}$$

and so if C_o is measured for a number of different span lengths, then a plot of $(C_o/N)^{1/3}$ versus L will yield the clamp correction from the negative L-axis intercept.

2.2.3 Corrected beam theory with effective crack length

Equation (7) can be re-arranged to solve for $a+\Delta_{II}$, which we refer to here as the calculated crack length, a_c, thus:

$$a_c = a + \Delta_{II} = \left[\frac{1}{3}\left\{\frac{2bh^3 E_1 C}{N} - (L + \Delta_{clamp})^3\right\}\right]^{\frac{1}{3}} \tag{9}$$

The value of the calculated crack length, a_c, may then be used in place of $(a+\Delta_{II})$ in equation (6) and the resulting equation (10) becomes independent of the measured crack length:

$$G_{IIC} = \frac{9P^2 a_c^2}{4b^2 h^3 E_1} \cdot F \tag{10}$$

Equation (10) is referred to here as the *Corrected Beam Theory with Effective Crack Length*, the (CBTE) method. The correction factor F in equation (10) is determined using the calculated crack lengths rather than the measured values. The analyses presented here all require that the value of the flexural modulus, E_1, be known for the specimen. If it is not known, then a flexural modulus test has to be performed prior to mode II testing. The use of equation (10) to determine G_{IIC} has the additional advantage that a value for Δ_{II} is not required *a-priori* and therefore, equation (5) need not be used. However, if Δ_{II} is deduced from equation (5), then an effective crack length, a_e, may be obtained via $a_e = a_c - \Delta_{II}$, and these values may be compared to the measured values of crack length to estimate or imply a crack length measurement error.

2.3 Experimental Compliance Method

The ESIS protocol [20] also uses a compliance calibration analysis method based upon the cubic relationship between the compliance, C and the measured crack length, a:

$$C = C_o + ma^3 \tag{11}$$

where C_o and m are constants. This approach is analogous to simple beam theory, but with the terms experimentally determined. Equation (11) may be differentiated and substituted into equation (2) to give:

$$G_{IIC} = \frac{3P^2a^2m}{2b} \cdot F \tag{12}$$

which is corrected for the effects of large displacements as before. Equation (12) is referred to as the 'Experimental Compliance Method' (ECM) in the present work. It is shown later that errors in the measured values of crack length have a significant effect upon the accuracy of this analysis method and it is more sensitive to crack length errors than beam theory analyses.

3. Experimental Procedures

3.1 Joint manufacture

The joints were manufactured using unidirectional carbon-fibre reinforced composite (T300/924 composite from Hexcel, UK.) as substrates. These were cut into beams 170mm long and nominally 20mm wide and 2mm thick. The height of each substrate was measured at three positions along their length using a micrometer and the average value recorded. The substrates were dried out in an oven to remove all moisture before bonding. The beams were abraded using 180/220 mesh alumina grit and were then solvent wiped. The substrates were then bonded with one of two adhesives. The first was a rubber toughened epoxy-paste adhesive, ESP110 from Permabond, UK. For these joints, cure was effected by clamping the joints in a bonding jig and holding the joints at 150°C for 45 minutes. The second adhesive was a rubber toughened epoxy-film adhesive, AF126 from 3M Inc, USA. In this case, cure was achieved by holding the joints in the clamping jig at 90°C for 90 minutes and then 120°C for 120 minutes. The bondline thickness was controlled using wire spacers or glass ballotini. To determine the bondline thickness, a micrometer was used to measure the total joint thickness at three positions along the length of the joint after curing and the average thickness of the two substrates used to make the joint were then subtracted from the joint thickness to give the thickness of the adhesive layer. The bondline thickness values were 0.4±0.05mm for the epoxy-paste adhesive and 0.08±0.04mm for the epoxy-film adhesive. Prior to forming the joints, a release film of 12.5μm thick PTFE was inserted into the centre of the bondline at one end to create a crack starter. After curing, the sides of the joints were ground using a belt-sander to remove the excess adhesive. The width of each joint was then measured at three positions along their length using vernier callipers and the average values recorded.

3.2 Measurement of the clamp correction

The correction term Δ_{clamp} was determined by performing an inverse ELS test in which the cracked portion of the joint was held fully within the clamp, which was tightened to the same torque as was used in the fracture tests (8Nm). This level of torque was chosen because it was found to be sufficiently high to give rigid clamping but not high enough to cause compressive damage to the composite substrates. The beam was then loaded within the elastic range and the compliance measured. In the procedure followed here, a number of tests were performed on the same specimen at different values of free length, *L*, ranging from 150mm to 80mm. The results are presented and discussed in section 4.

3.3 Experimental fracture testing

Aluminium loading blocks of height 12.5mm and length 20mm were bonded onto the ends of the joints and one side of the joint was coated with a thin layer of water based type-writer correction fluid to facilitate visual determination of the crack length. Grid lines were then marked on the side on the sample at 1mm and then 5mm intervals. For the joints bonded with the epoxy-paste adhesive, the non-adhesive film initially extended 60mm from the centre of the loading block hole, and this was grown by 4-5mm during a mode I pre-cracking stage, as described in the British Standard for mode I testing [2]. This was performed to provide a sharp natural initial crack for the subsequent mode II test and to improve the test stability. For the joints bonded with the epoxy-film adhesive, the initial film length was 70mm from the loading line, and this was grown by 3-4mm during mode I pre-cracking.

The joints were then transferred to the mode II ELS test fixture. This incorporated a linear bearing trolley to allow free horizontal translation of the specimen during loading. The free-length, L, was set to 120mm for the joints bonded with the epoxy-paste adhesive and 130mm for joints bonded with the epoxy-film adhesive. Figure 3 shows a photograph of a joint being loaded in the fixture. The tests were run in displacement control at a rate of 1.0 mm/min. During the tests, the crack length was observed along the edge of the specimen using a travelling microscope with a magnification of X7. The load and the cross-head displacement were recorded at 5mm increments of observed crack growth, until the crack reached a length of 100mm for the joints bonded with the epoxy-paste adhesive or 115mm for the joints bonded with the epoxy-film adhesive. The test was then stopped and the specimen was fully unloaded and checked for any signs of any permanent plastic deformation. All tests remained fully elastic during the test. Some additional photographs were taken during tests on additional samples using a high magnification CCD camera to study in detail the behaviour at and around the measured crack tip. Full details of the experiments performed can be found in [21].

3.4 Measurement of the system compliance and specimen flexural modulus

The compliance of the test fixture was measured by clamping a very stiff calibration specimen in place of the test specimen, and loading the test system up to the loads obtained in the fracture tests. The system compliance measured was 1×10^{-4} mm/N. This value of system compliance was shown to be sufficiently small to have negligible effect on the results obtained. The flexural modulus of the substrate arms was determined on a number of composite beams prior to bonding, according to the ASTM standard for the determination of flexural properties of reinforced plastics [22]. The value of the modulus determined was 126±2 GPa, which was in excellent agreement with the value quoted by the manufacturer.

4. Results and Discussion

4.1 Results from the inverse ELS tests

From the inverse ELS tests performed, the values of $(C_o/N)^{1/3}$ were plotted against free length L. Results from a typical test are shown in Figure 4. These data were linear with the slope being proportional to $E_1^{-1/3}$ and the clamping correction Δ_{clamp} being deduced from the negative intercept with the L-axis. The values of Δ_{clamp} deduced from this procedure were typically between 4 and 6mm, i.e. about half the values that were deduced when the correction on L was determined from the mode I value, i.e. as shown in equation (4). This lower value reflected the different clamping condition when the specimens are clamped in the ELS fixture, as opposed to the clamping assumed at the crack tip in a mode I DCB test. The effect of the clamping correction on the predicted specimen compliance is discussed in the next section.

4.2 Results for joints bonded with the epoxy-paste adhesive

4.2.1 Force-versus displacement and compliance results

Figure 5 shows a typical force-displacement trace obtained from testing a joint bonded with the epoxy-paste adhesive. The initial crack length in the mode II test was 65mm and this was grown to 100mm during the test. Unloading was performed from 100mm, with the trace returning to the origin, confirming that the substrate arms were not permanently deformed during the test. The visually determined values of crack length are shown on the graph.

The ESIS test protocol for the determination of G_{IIC} for fibre-composite laminates [20], in common with the standard for the determination of G_{IC} for structural adhesives [2] specifies three ways to determine crack initiation. The first, termed the non-linear (NL) point is when the initial loading first deviates from linearity. For these tests, this point was identified on the machine chart with a very much magnified displacement axis. The second initiation point is the point determined by the operator whilst viewing the side of the joint through the microscope. This is termed the visual (VIS) initiation point. For the third initiation point, the slope of the initial compliance line is reduced by 5% and initiation is defined as the point of intersection between this line and the loading curve. However, if this intersection occurs after the maximum load point, then the maximum load point is used instead, so the point is the 5% compliance offset or maximum load point, whichever occurs first. For these tests, the 5% offset point always preceded the maximum load point. All other points on the graph in Figure 5 are propagation points, i.e. are identified as points by the operator when the crack is observed to pass through a grid line marked on the specimen edge.

All tests resulted in stable, cohesive crack growth within the adhesive layer. The load, displacement and visually determined crack length data were entered into a 'Microsoft Excel' spreadsheet for data analysis as outlined in Section 2 above. The value for E_1 was taken as 126GPa from the flexural modulus tests and the value of Δ_{clamp} was taken as 5.8mm from the inverse ELS test. The value of Δ_{II} was deduced from equation (5) using the values of Δ_I measured in mode I DCB tests as reported in [21]. The value of Δ_I was approximately the same for the two joint types and a constant value of 6mm was used for the determination of Δ_{II} in equation (5).

To establish the accuracy of the various analyses presented in Section 2, the experimentally determined values of compliance ($C=\delta/P$) were compared to the analytically predicted values. The values of compliance were determined as a function of the cube of the measured crack length, a^3, via Simple Beam Theory, equation (1) and via Corrected Beam Theory, equations (4) and (7). These values are shown in Figure 6 for the experimental test data presented in Figure 5. Figure 6 shows that the values of compliance predicted by the Simple Beam Theory, i.e. equation (1), are a poor fit to the experimental data (shown as filled points in the figure). This reflects the importance of the various correction factors described in Section (2). Deducing the compliance via the Corrected Beam Theory of equation (4) is also a poor fit to the experimental data. The error is caused by the over-correction when L was corrected by $2\Delta_I$. The Corrected Beam Theory of equation (7) was the best fit to the experimental data, i.e. when the experimentally-determined clamp correction, Δ_{clamp}, was used. It should be noted that Δ_{II} was still determined via equation (5) for use in equation (7) and hence this approach appears to be relatively satisfactory. The experimental data show some scatter but on the whole fit to equation (7) quite accurately, confirming the soundness of the approach in this case.

4.2.2 Crack length measurements

Next, the values of the crack length, a, were compared to the values calculated, a_c, via equation (9), and the effective values, a_e, that were then determined via $a_e = a_c - \Delta_{II}$. These values are shown for two repeat tests in Table 1. The implied error in measured crack length is given by (a-a_e) and the average error was -1.4mm for the first test and +1.4mm for the second test. The error values show a random behaviour, implying that that for these joints the crack length measurements were not subject to any systematic errors which may have been induced had the operator been misled by microcracking of the adhesive layer.

4.2.3 Values of G_{IIC}

The various analysis schemes were then used to determine the values of G_{IIC} as a function of measured crack length, i.e. to construct the resistance curve (R-curve). The values of G_{IIC} deduced for the second test in Table 1 are shown in Table 2. Regardless of the analysis method used, the lower bound values of G_{IIC} were always given by the non-linear initiation points, and then a pronounced rising R-curve was always observed, reaching a more or less stable, plateau, region of approximately constant G_{IIC} after some 10mm of crack propagation. The values of G_{IIC} associated with all measured crack lengths also are shown in Figure 7. To facilitate comparison of the propagation results, it is useful to define, for each analysis method, a single value of G_{IIC} from the propagation plateau region. In the present work, a 'mean plateau' value of G_{IIC} has been defined as the arithmetic mean of the G_{IIC} values recorded over the plateau region (i.e. over the part of the R-curve with approximately constant values of G_{IIC}). In Table 2, this was determined as being from a=75mm to a=100mm.

The simple beam theory, equation (3), returned similar, but higher values of G_{IIC} than the corrected beam theory of equation (6). The increase due to the correction to the crack length, Δ_{II}, was more than offset by the large displacement correction factor, F, which was typically in the range of 1.0 to 0.9 for these tests. The values of G_{IIC} deduced via the corrected beam theory with effective crack length (CBTE) theory, equation (10), was below that predicted via the corrected beam theory of equation (6). On average, a value of Δ_{II}=0.97mm would have been required in equation (6) to yield the results predicted by the CBTE method. Note that Δ_{II} =2.4mm was obtained using equation (5) and used in equation (6). It is noteworthy also that the values of G_{IIC} deduced via the experimental compliance approach, whilst showing a similar form, were lower than all beam theory values in these tests.

The mean and standard deviation values of G_{IIC} for four repeat tests, expressed as the coefficient of variation, are shown Table 3. Values deduced via equations (3), (6), (10) and (12) are shown. As discussed above, the values obtained via the experimental compliance method (ECM) are the lowest and the corrected beam theory methods are all in close agreement. The non-linear initiation values were significantly below the values obtained via the visual or 5% offset definitions. The mean plateau value of G_{IIC} at about 4500 J/m^2 was about twice the visual initiation value. The effect of using a_e rather than a in the experimental compliance approach was investigated, and values of G_{IIC} determined via the use of both a and a_e are shown in Tables 2 and 3. It is seen that for joints bonded with the epoxy-paste adhesive there was no significant difference in the values obtained, unlike the joints bonded with the epoxy-film adhesive which are discussed next.

4.3 Results for the joints bonded with the epoxy-film adhesive

4.3.1 Force versus displacement and compliance results

A typical force-displacement trace for a joint bonded with the epoxy-film adhesive is shown in Figure 8. It was noteworthy that the trace deviated from linearity at 45% of the maximum load value and that a significant extent of crack propagation was observed prior to the maximum load being attained. Following this maximum, there was a quite abrupt change of slope. The 5% offset initiation point occurred after the crack had appeared to pass through the first three crack propagation grid lines.

The experimentally determined values of compliance for this test were compared to the analytically predicted values as described previously. Figure 9 shows these data, which was typical for the joints bonded with the epoxy-film adhesive. It is clear from the figure that the experimental compliance rises only very slowly for the first 10-15mm of measured crack growth, i.e. from a=74mm to about a=90mm in Figure 9. Then the slope of the C versus a^3 line increases. The most probable explanation for this observation is that the test operator has been misled by the initiation and development of microcracks along the specimen edge, and has mistakenly recorded this as main crack growth. These microcracks have little effect on measured compliance and it can be seen that the initial compliance is predicted accurately at the initial crack length, a_o, using the corrected beam theory of equation (7). The experimental compliance values then begin to rise but do so approximately along a line translated by 10-15mm (which is then cubed in Figure 9) to the line predicted by equation (7).

4.3.2 Crack length measurements

Figure 10 shows two photographs which were taken during the testing of a joint bonded with the epoxy-film adhesive. The two vertical black lines in Figure 10(a) were drawn 1mm apart and the inclined horizontal lines on the photograph indicate the position of the adhesive/substrate interfaces and hence define the position of the adhesive layer. Microcracks can be seen inclined at approximately 45° to the specimen axis, extending for several mm in length and across the entire bondline height. Figure 10(b) shows these microcracks coalescing towards the left of the picture (at the shorter crack length) and forming a continuous crack along the upper (compressive) interface. The definition of the *true* crack length in this situation is unclear and is certainly an issue which the current test protocols do not address. However, the idea and use of the calculated, a_c, and hence effective, a_e, crack lengths is particularly valuable in these tests.

The values of the calculated crack length, a_c, the effective crack length, a_e and the measured crack length, a, are shown in Table 4 for the two repeat tests on the joints bonded with the epoxy-film adhesive. Again, the implied crack length error is given by (a-a_e) and this error rises from crack initiation to an average value of approximately +7mm during crack propagation in each test. This error is incurred within the first 10mm of apparent measured crack growth. Such implied errors are consistent with the notion that microcracking has been mistaken as main crack growth by the test operator. (The values of a_c and a_e are derived from the specimen compliance and are thus independent of the crack length measurement errors.)

4.3.3 Values of G_{IIC}

Values of G_{IIC} were then deduced for each test using the various analysis schemes. These values, calculated for each crack length, are shown in Figure 11 and table 5 for the test data presented in Figures 8 and 9. The values of G_{IIC} deduced show the same basic form for each analysis method. The non-linear initiation value is the lower bound value with the 5% offset being the upper bound initiation value. The SBT approach returns very similar results to the CBT approach via equation (6), in which Δ_{II} was deduced from equation (5) and was approximately 2.5mm for these joints. However, the values deduced using the CBTE method were some 10% lower, due to the lower values of a_c relative to the measured crack lengths, a.

The experimental compliance method, equation (12), has resulted in the lowest G_{IIC} values when the measured compliance was plotted against the cube of the measured crack length (shown as ECM (with a) in Table 5). The use of the effective crack length, a_e, in the compliance calibration, equation (11) and in equation (12) results in higher values (closer to those produced via the CBTE method). This highlights the extreme sensitivity of the experimental compliance analysis approach to measurement errors in the crack length. The resistance curve (Figure 11) shows an abrupt change of slope at 90mm which corresponds to the onset of main crack growth as identified in Figure 11. The main values are summarised for the four repeat tests in Table 6.

4.4 General Observations

In the corrected beam theory analysis of (§2.2.1) the accuracy of the correction to the free length, L is not important because, as it is a constant, it does not affect the values of dC/da and hence it does not affect the values of G_{IIC} deduced. However, in the effective crack length approach (§2.2.3) the free length correction is clearly important because the accuracy of the calculated crack lengths are dependant upon this correction. The procedure followed in the present work has resulted in quite accurate predictions of the specimen compliance during mode II testing of the joints bonded with the epoxy-paste adhesive, when the crack lengths were accurately measured. This confirms the general soundness of this correction procedure.

For the joints bonded with the epoxy-paste adhesive, the non-linear initiation value of G_{IIC} was approximately equivalent to the value of G_{IC} measured using the double cantilever beam test specimen, see Table 3. For the joints bonded with the epoxy-film adhesive, the mode I value was closer to the 5% offset definition value of G_{IIC} initiation, see Table 6. From the previous discussion, the visual definition of initiation for this adhesive joint was erroneous due to the misinterpretation of microcracking as main crack growth. In addition, the extensive microcracking may well have caused the non-linear point also to have preceded the true initiation point. Thus, whilst there is some evidence that G_{IC} is equivalent to a mode II crack initiation, i.e. to a G_{IIC} (initiation) value, such a relationship has yet to be conclusively established.

The strongly rising R-curve behaviour demonstrated by the joints is noteworthy. The elevations in the values of G_{IIC} would appear to originate from the development of the characteristic damage mechanism involving the initiation and propagation of inclined microcracks [23, 24]. If the microcracks extend across the entire height of the bond-line as was clearly observed in the thinner epoxy-film adhesive layer, then the enhancement in fracture surface area for 45° microcracks can be approximated by $\sqrt{2}(h_a / d)$ where h_a is the bond-line thickness and d is the spacing between microcracks. For joints bonded with the epoxy-film adhesive, h_a was 0.08mm and d was of the order of 0.045mm, implying an area enhancement of about 2.5 times. For the mean plateau value of G_{IIC} via the CBTE method in Table 6 of 3381 J/m^2, this would suggest a G_{IIC} initiation value of 1353 J/m^2, which is indeed between the values obtained via the visual and 5% offset definitions of crack initiation. This is also in good agreement with the G_{IC} value of 1449 $\pm$ 113 J/m^2. The high magnification photography of the joints bonded with the thicker layer of epoxy-paste adhesive indicated that the inclined microcracks did not extend across the entire height of the bond-line, but were localised in the adhesive layer close to the compressive interface. The area enhancement therefore does not necessarily appear to scale with bond-line thickness.

Finally, it is clearly of interest to note that, whilst the complex damage mechanism was observed to occur within both joint types, the effective crack length analysis has only predicted significant crack length measurement errors occurred when testing the joints bonded with the epoxy-film adhesive, where the damage mechanism of microcracking was more clearly evident and appeared to be a far more major problem.

5. Conclusions

The end-loaded split (ELS) test was employed for the determination of G_{IIC} in adhesive joints consisting of carbon-fibre reinforced composite substrates bonded with one of two structural epoxy adhesives. A number of analysis schemes were examined for the determination of the compliance, and then G_{IIC}, as a function of the measured crack growth in the tests. The uncorrected simple beam theory (SBT) analysis approach was shown to give a poor fit to the experimental compliance data, indicating the importance of the various correction factors to beam theory which were considered. These included length corrections to the clamped free length of the specimen and to the measured crack length, and also two finite displacement corrections factors which had been reported previously. It was shown that the compliance calculated by the corrected beam theory approach was very sensitive to the clamped free length correction and that deducing the value of this correction from mode I test data (as had previously been suggested) was unreliable, leading to an over-correction to the data in this case. Deducing this correction from an inverse ELS test, in which the cracked section of the joint was held fully inside the clamp, was shown to yield correction values which, when combined with beam theory, predicted the measured specimen compliance quite accurately. The analytical compliance from the corrected beam theory (CBT) approach was used to back-calculate the values of crack length for the ELS tests. An effective crack length was then deduced from the calculated value and this permitted an assessment of the accuracy of the measured crack lengths, as these values could be compared to the effective values. Also, an additional scheme for the determination of G_{IIC} was defined, based upon the effective crack lengths, termed the corrected beam theory with effective crack length (CBTE) approach.

For the joints bonded with the epoxy-paste adhesive, the corrected beam theory analysis approach closely predicted the measured specimen compliance values, confirming the validity of this analysis method and its applicability to adhesively bonded joints. The effective crack lengths were also shown to be in close agreement with the measured values and so the values of G_{IIC} deduced via the CBT and CBTE approaches were similar, as would be expected. However, for the joints bonded with the epoxy-film adhesive, the CBT approach failed to predict the measured specimen compliance after crack initiation. The effective crack length calculation showed that errors had been made in the measurement of crack length for these joints, due to misinterpreting microcracking as main crack growth. These crack length errors had a large effect on the values of G_{IIC} deduced via both the CBT and experimental compliance method (ECM) approaches.

Considering the initiation values of G_{IIC}, the joints bonded with the epoxy-paste adhesive exhibited non-linear initiation values close to the value of G_{IC}, but the visual and 5% offset definition values were at least twice this value. The joints bonded with the epoxy-film adhesive exhibited non-linear values well below the value of G_{IC} but the visual and 5% offset definitions were close to the G_{IC} value. Both adhesive types exhibited strongly rising R-curve behaviour following crack initiation. The values of G_{IIC} then showed a region of approximately constant value, which allowed a 'plateau' value to be defined. The rising R-curve was considered to be most likely the result of the inclined microcracks which formed ahead of the main crack in the adhesive layer. A simple calculation of the enhancement in fracture surface area generated by this damage mechanism predicted an enhancement of 2.5 times for the epoxy-film adhesive. The actual increase in the value of G_{IIC} from the 5%

definition value to the plateau was close to this, supporting the idea that the rising G_{IIC} values were mainly caused by the enhancement in fracture surface area. Finally, and particularly when microcracking was occurring, an analysis scheme based upon an effective crack length, which is independent of measured crack length, would appear more robust.

Acknowledgements

We wish to thank the Engineering and Physical Sciences Research Council (EPSRC) for an Advanced Fellowship (AF/992781) and Platform Grant, and the National Physical laboratory (NPL) for funding the PhD studentship of Marion Paraschi. Also, we wish to thank Professor J.G. Williams for the valuable discussions on the ideas presented here, and the ESIS TC4 technical committee.

References

1. Blackman, B.R.K., Kinloch, A.J., Paraschi, M. and Teo, W.S., *Measuring the mode I adhesive fracture energy, G_{IC}, of structural adhesive joints: The results of an International round-robin.* International Journal of Adhesion and Adhesives, 2003. **23**: p. 293-305.
2. BSI, *Determination of the mode I adhesive fracture energy, G_{IC}, of structural adhesives using the double cantilever beam (DCB) and tapered double cantilever beam (TDCB) specimens.* 2001. **BS 7991**.
3. Kinloch, A.J., *Adhesion & Adhesives: Science & Technology*. 1987, London & New York: Chapman Hall. 441.
4. Martin, R.H. and B.D. Davidson, *Mode II fracture toughness evaluation using four point bend, end notched flexure test.* Plastics, Rubber and Composites, 1999. **28**(8): p. 401-406.
5. Qiao, P., J. Wang, and J.F. Davalos, *Analysis of tapered ENF specimen and characterization of bonded interface fracture under Mode II loading.* International Journal of Solids & Structures, 2003. **40**: p. 1865-1884.
6. Edde, F.C. and Y. Verreman, *Nominally constant strain energy release rate specimen for the study of mode II fracture and fatigue in adhesively bonded joints. International Journal of Adhesion and Adhesives, 1995,* ***15***: p. *29-32.*

7. Davies, P., et al., *Comparison of test configurations for determination of mode II interlaminar fracture toughness results from international collaborative test programme.* Plastics, Rubber and Composites, 1999. **28**(9): p. 432-437.
8. Carlsson, L.A., J.W. Gillespie, and R.B. Pipes, *On the analysis and design of the end notched flexure (ENF) specimen form mode II testing.* Journal of Composite Materials, 1986. **20**: p. 594-604.
9. Russel, A.J. and K.N. Street. *Factors affecting the interlaminar fracture energy of graphite/epoxy laminates*. in *ICCM-IV*. 1982. Tokyo, Japan.
10. Fernlund, G. and J.K. Spelt. *Mixed-mode fracture characterisation of adhesive joints. Composites Science and technology, 1994,* ***50****: p441-449.*
11. Schuecker, C. and B.D. Davidson, *Effect of friction on the perceived mode II delamination toughness from three and four point bend end-notched flexure tests*, in *Composites Structures: Theory and Practice,* P. Grant and C.Q. Rousseau, Editors. 2000, American Society of Testing and Materials: West Conshohocken. p. 334-344.
12. Schuecker, C. and B.D. Davidson, *Evaluation of the accuracy of the four-point bend end-notched flexure test for the mode II delamination toughness determination.* Composites Science and Technology, 2000. **60**: p. 2137-2146.
13. Davies, P., *Influence of ENF specimen geometry and friction on the mode II delamination resistance of cardon/PEEK.* Journal of Thermoplastic Composite Materials, 1997. **10**: p. 353-361.
14. Blackman, B.R.K. and J.G. Williams. *On the mode II testing of carbon-fibre polymer composites*. in *ECF12 Fracture from Defects*. 1998. Sheffield, UK: EMAS publishing.
15. Brunner, A.J., *Experimental aspects of mode I and mode II fracture toughness testing of fibre-reinforced polymer-matrix composites.* Computer Methods in Applied Mechanics and Engineering, 2000. **185**: p. 161-172.
16. Brunner, A.J., B.R.K. Blackman, and J.G. Williams, *Calculating a damage parameter and bridging stress from* G_{IC} *delamination tests on fibre composites.* Composites Science and Technology, 2004. **in press 2004**.
17. Brunner, A.J., B.R.K. Blackman, and J.G. Williams. *Deducing bridging stresses and damage from* G_{IC} *tests on fibre composites*. in *Fracture of Polymers, Composites and Adhesives II*. 2002. Les Diablerets, Switzerland: Elsevier Science Ltd.
18. Hashemi, S., A.J. Kinloch, and J.G. Williams, *The analysis of interlaminar fracture in uniaxial fibre-polymer composites.* Proceeding of the Royal Society London, 1990. **A427**: p. 173-199.

19. Wang, Y. and J.G. Williams, *Corrections for mode II fracture toughness specimens of composite materials.* Composites Science and Technology, 1992. **43**: p. 251-256.
20. Davies, P., B.R.K. Blackman, and A.J. Brunner, *Mode II delamination,* in *Fracture mechanics testing methods for polymers adhesives and composites*, D.R. Moore, A. Pavan, and J.G. Williams, Editors. 2001, Elsevier: Amsterdam, London, New York. p. 307-334.
21. Paraschi, M., *A fracture mechanics approach to the failure of adhesive joints*, in *Department of Mechanical Engineering*. 2002, Imperial College, University of London: London.
22. ASTM, *Determination of flexural properties of plastics and reinforced plastics*. 1990.
23. O'Brien, T.K., *Composite interlaminar shear fracture toughness, G_{IIC}: Shear measurement or sheer myth?,* in *Composite Materials: Fatigue and Fracture*. 1998. p. 3-18.
24. Lee, S.M., *Mode II delamination failure mechanisms of polymer matrix composites.* Journal of Materials Science, 1997. **32**: p. 1287-1295.

Appendix 1.

$$F = 1 - \theta_1 \left(\frac{\delta}{L}\right)^2 - \theta_2 \left(\frac{\delta l_1}{L^2}\right) \tag{A1}$$

$$N = 1 - \theta_3 \left(\frac{l_2}{L}\right)^3 - \theta_4 \left(\frac{\delta l_1}{L^2}\right) - \theta_5 \left(\frac{\delta}{L}\right)^2 \tag{A2}$$

$$\theta_1 = \frac{3}{20}\left[\frac{15 + 50\left(\frac{a}{L}\right)^2 + 63\left(\frac{a}{L}\right)^4}{1 + 3\left(\frac{a}{L}\right)^3}\right]^2 \tag{A3}$$

$$\theta_2 = \frac{-3\left(\frac{L}{a}\right)\left(1 + 3\left(\frac{a}{L}\right)^2\right)}{1 + 3\left(\frac{a}{L}\right)^3} \tag{A4}$$

$$\theta_3 = \frac{4}{1 + 3\left(\frac{a}{L}\right)^3} \tag{A5}$$

$$\theta_4 = \frac{-9}{4}\frac{\left[\left(1 - \left(\frac{a}{L}\right)\right)\left(1 + 3\left(\frac{a}{L}\right)^3\right) + 4\left(\frac{a}{L}\right)^2\left(1 - \left(\frac{l_2}{a}\right)^2\right)\left(1 + 3\left(\frac{a}{L}\right)^2\right)\right]}{\left(1 + 3\left(\frac{a}{L}\right)^3\right)^2} \tag{A6}$$

$$\theta_5 = \frac{36}{35} \cdot \frac{1 + \frac{3}{8}\left(\frac{a}{L}\right)^3\left(35 + 70\left(\frac{a}{L}\right)^2 + 63\left(\frac{a}{L}\right)^4\right)}{\left(1 + 7\left(\frac{a}{L}\right)^3\right)^3} \tag{A7}$$

TABLES

Table 1. Values of calculated, a_c, effective, a_e, and measured crack lengths, a, for two joints bonded with the epoxy-paste adhesive. Implied crack length errors are also given (all values in mm).

Test 2				Test 3			
a_c	a_e	a	*error*	a_c	a_e	a	*error*
62.8	60.4	64.0	3.6	63.0	60.6	65.0	4.4
69.4	67.0	64.0	-3.0	65.4	63.0	65.0	2.0
68.7	66.3	64.0	-2.3	68.2	65.8	65.0	-0.8
69.7	67.2	66.0	-1.2	66.2	63.8	67.0	3.2
70.4	68.0	67.0	-1.0	68.8	66.4	68.0	1.6
72.3	69.8	68.0	-1.8	70.3	67.9	69.0	1.1
72.8	70.3	69.0	-1.3	71.5	69.1	70.0	0.9
73.3	70.8	70.0	-0.8	77.1	74.7	75.0	0.3
79.6	77.2	75.0	-2.2	80.9	78.5	80.0	1.5
85.1	82.7	80.0	-2.7	85.6	83.2	85.0	1.8
90.7	88.2	85.0	-3.2	91.2	88.8	90.0	1.2
92.7	90.3	90.0	-0.3	94.0	91.6	95.0	3.4
97.9	95.4	95.0	-0.4	97.7	95.3	97.0	1.7
100.7	98.3	98.0	-0.3	100.1	97.7	98.0	0.3
104.2	101.7	100.0	-1.7	102.2	99.8	100.0	0.2
	Average* error in *a*		-1.4		Average* error in *a*		1.4

Notes: a_c is the calculated crack length via equation (9); a_e is the effective crack length deduced via (a_c-Δ_{II}); a is the experimentally measured crack length; error is (a-a_e); (*) is the average of the propagation values, i.e. the first three rows of data are not included in the calculation)

Table 2. Values of G_{IIC} calculated via the various analysis schemes (see text for details) for a joint bonded with the epoxy-paste adhesive (Test 3).

a	G_{IIC} (J/m^2)				
(mm)	SBT eqn. (3)	CBT eqn. (6)	CBTE eqn. (10)	ECM (with *a*) eqn (12)	ECM (with a_e) eqn (12)
(NL) 65	1126	1227	1072	985	873
(VIS) 65	2204	2356	2218	1891	1811
(5 %) 65	2721	2866	2928	2300	2398
67	2609	2763	2516	2222	2056
68	3180	3315	3169	2669	2598
69	3488	3605	3495	2905	2869
70	3935	4020	3917	3242	3219
(p) 75	5216	5141	5103	4165	4214
(p) 80	5771	5614	5414	4566	4485
(p) 85	5976	5763	5527	4703	4594
(p) 90	6047	5772	5634	4725	4699
(p) 95	6326	6025	5611	4946	4688
(p) 97	6059	5744	5560	4720	4655
(p) 98	5779	5471	5454	4497	4571
(p) 100	5812	5482	5473	4511	4592
Mean Plateau	5873	5627	5472	4604	4562

Notes: P →Plateau region (*a*=75mm to *a*=100mm) in this test.

Table 3. Mean values of G_{IIC} at crack initiation and for 'mean plateau' for joints bonded with the epoxy-paste adhesive. Mean and coefficients of variation in (%) of four tests are shown.

	G_{IIC} (J/m^2)				
Value	SBT (Eqn. 3)	CBT (Eqn. 6)	CBTE (Eqn. 10)	ECM (with a) (Eqn. 12)	ECM (with a_e) (Eqn. 12)
NL	1045 (26%)	1140 (26%)	1029 (31%)	950 (23%)	887 (33%)
VIS	2075 (15%)	2223 (15%)	2250 (19%)	1866 (15%)	1946 (21%)
Max/5%	2378 (17%)	2523 (16%)	2672 (20%)	2107 (13%)	2313 (21%)
Mean plateau	4679 (15%)	4597 (13%)	4280 (3%)	3925 (10%)	3976 (9%)

G_{IC} via BS7991: 945±28 J/m^2.

Table 4. Values of calculated, a_c, effective, a_e, and measured crack lengths, a, for two joints bonded with the epoxy-film adhesive. Implied crack length errors are also given (all values in mm).

Test 3				Test 4			
a_c	a_e	a	*error*	a_c	a_e	a	*error*
73.2	70.7	74.0	3.3	74.4	71.9	74.0	2.1
75.1	72.6	74.0	1.4	76.5	74.0	74.0	0.0
80.3	77.8	74.0	-3.8	79.7	77.2	74.0	-3.2
76.5	74.0	79.0	5.0	76.1	73.6	77.0	3.4
76.6	74.1	80.0	5.9	78.6	76.1	79.0	2.8
79.6	77.1	85.0	7.9	77.9	75.4	80.0	4.6
81.5	79.0	90.0	11.0	80.1	77.6	85.0	7.3
88.2	85.7	95.0	9.3	82.4	79.9	90.0	10.1
95.7	93.3	100.0	6.7	91.7	89.2	95.0	5.8
100.7	98.2	105.0	6.8	95.0	92.5	100.0	7.5
105.4	102.9	110.0	7.1	98.4	95.9	105.0	9.1
108.9	106.4	114.0	7.6	103.0	100.5	110.0	9.5
110.3	107.8	115.0	7.2	107.8	105.3	115.0	9.7
	Average* error in *a*		+7.4		Average error in *a*		+7.0

Notes: a_c is the calculated crack length via equation (9); a_e is the effective crack length deduced via (a_c-Δ_{II}); *a* is the experimentally measured crack length; error is (a-a_e); (*) is the average of the propagation values, i.e. the first three rows of data are not included in the calculation)

Table 5. Values of G_{IIC} calculated via the various analysis schemes (see text for details) for a joint bonded with the epoxy-film adhesive (Test 4).

a	G_{IIC} (J/m^2)				
(mm)	SBT eqn. (3)	CBT eqn. (6)	CBTE eqn. (10)	ECM (with *a*) eqn (12)	ECM (with a_e) eqn (12)
(NL) 74	460	499	471	316	410
(VIS) 74	626	678	677	429	590
(5%) 74	1316	1406	1522	890	1330
77	768	827	759	525	661
79	1052	1126	1049	716	916
80	1250	1334	1191	849	1040
85	2040	2142	1798	1367	1573
90	3194	3284	2604	2104	2281
95	3423	3462	3060	2224	2698
100	3558	3586	3075	2309	2716
105	3704	3718	3108	2400	2751
110	3733	3732	3118	2414	2766
115	3836	3812	3193	2471	2838
Mean Plateau	3575	3599	3111	2320	2754

Table 6. Mean values of G_{IIC} at crack initiation and for 'mean plateau' for joints bonded with the epoxy-film adhesive. Mean and coefficients of variation in (%) of four tests are shown.

	G_{IIC} (J/m^2)				
Value	SBT (Eqn. 3)	CBT (Eqn. 6)	CBTE (Eqn. 10)	ECM (with a) (Eqn. 12)	ECM (with a_e) (Eqn. 12)
NL	553 (24%)	598 (23%)	559 (22%)	420 (27%)	477 (21%)
VIS	474 (27%)	807 (27%)	788 (26%)	567 (30%)	675 (25%)
Max/5%	1404 (30%)	1482 (29%)	1624 (32%)	1036 (31%)	1391 (31%)
Mean plateau	3921(12%)	3892 (11%)	3381 (11%)	2774 (14%)	2943 (9%)

G_{IC} via BS7991: 1449+113J /m^2

(a)

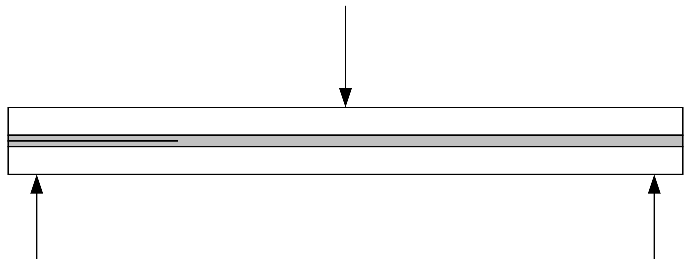

(b)

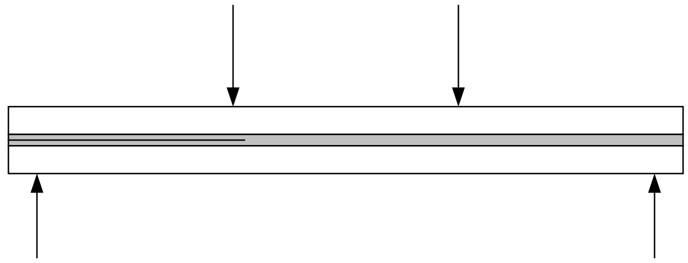

(c)

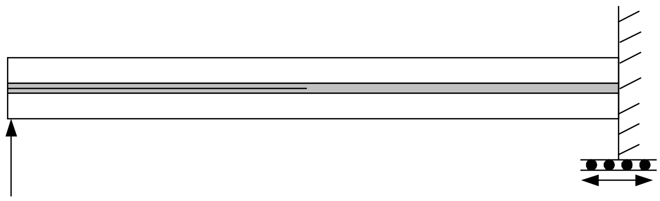

(d)

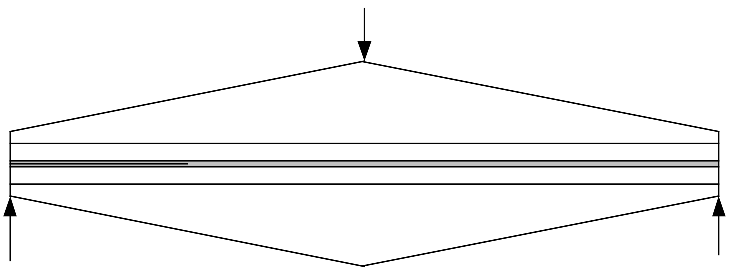

Figure 1. Mode II test configurations. (a) The 3-point end-notched flexure (ENF) test, (b) the 4-point end-notched flexure (4-ENF) test, (c) the end-loaded split (ELS) test and (d) the tapered end-loaded split (TENF) test.

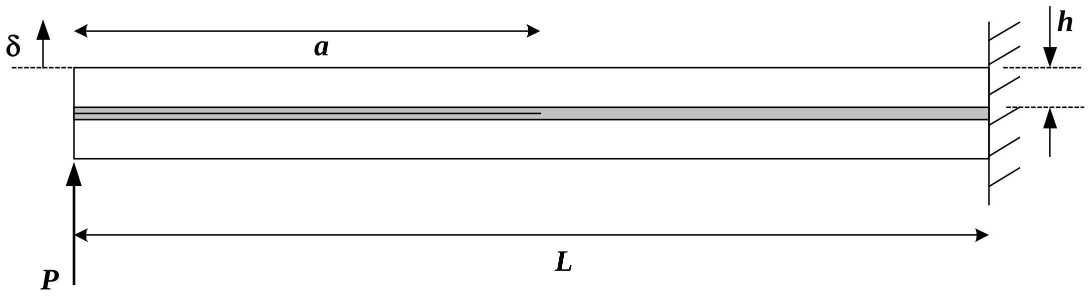

Figure 2. Schematic diagram of the ELS test specimen with parameters defined.

Figure 3. The end-loaded split (ELS) test fixture and adhesive joint specimen.

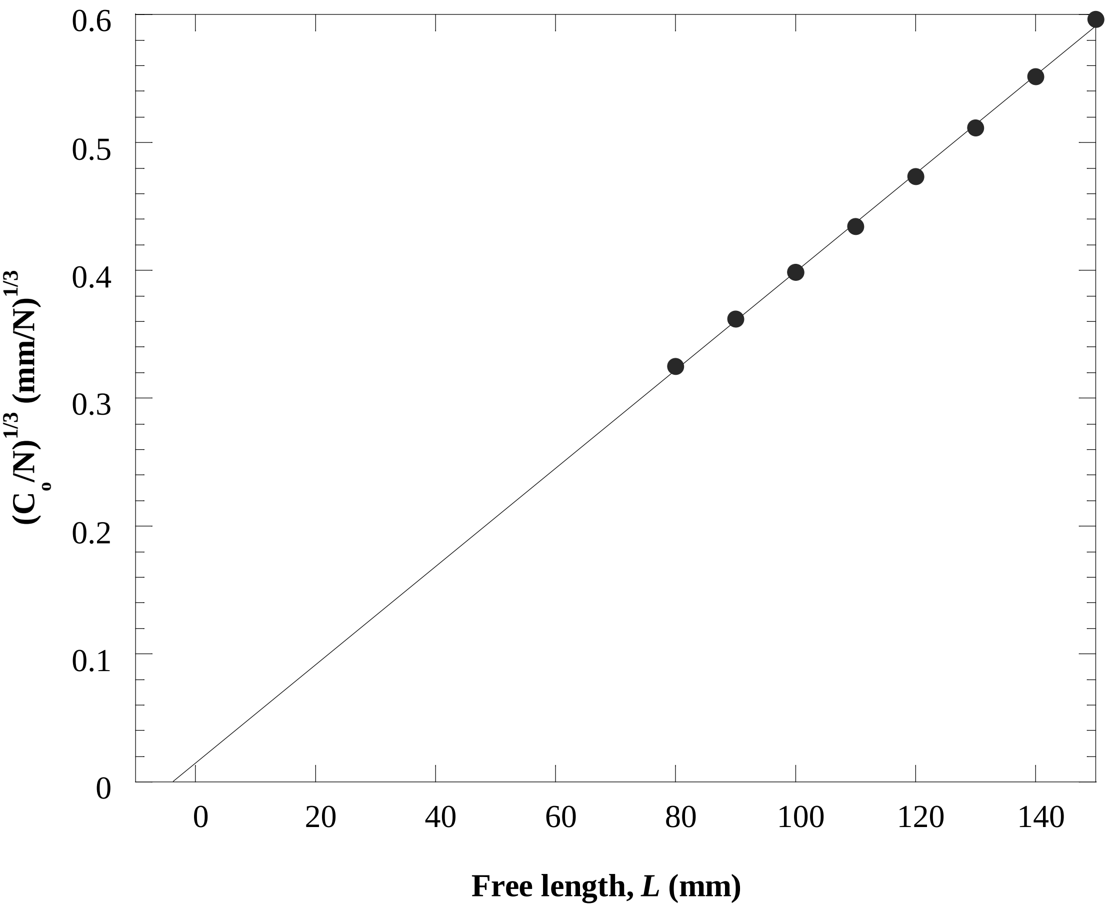

Figure 4. Graph of $(Co/N)^{1/3}$ versus free length, L, measured during the inverse ELS (IELS) tests for the determination of the clamp correction Δ_{clamp}. (Note that Δ_{clamp} is the (-)ve L-axis intercept).

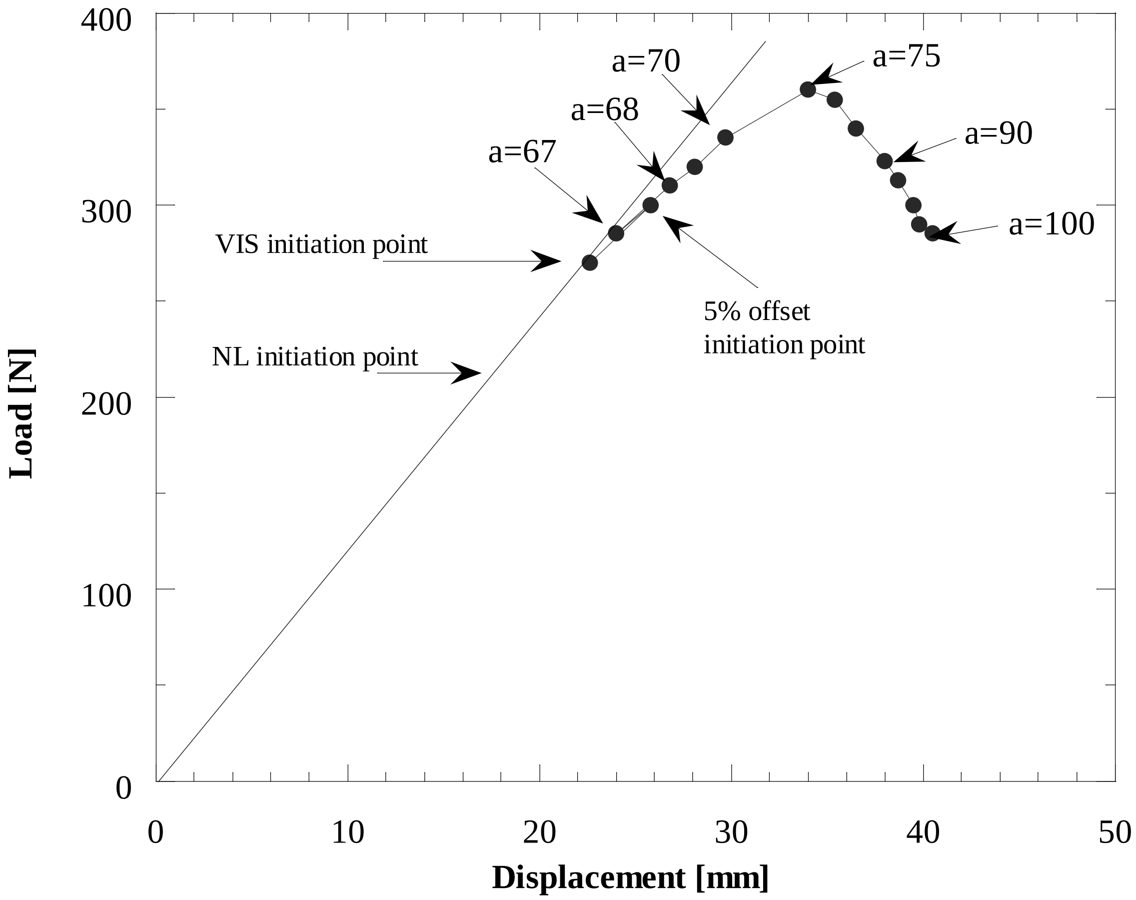

Figure 5. Typical force-displacement trace for a joint bonded with the epoxy-paste adhesive. (**Notes: (1) Measured crack length, *a*, values shown are in mm, (2) The non-linear (NL) initiation point was defined on a machine chart with a magnified displacement axis**).

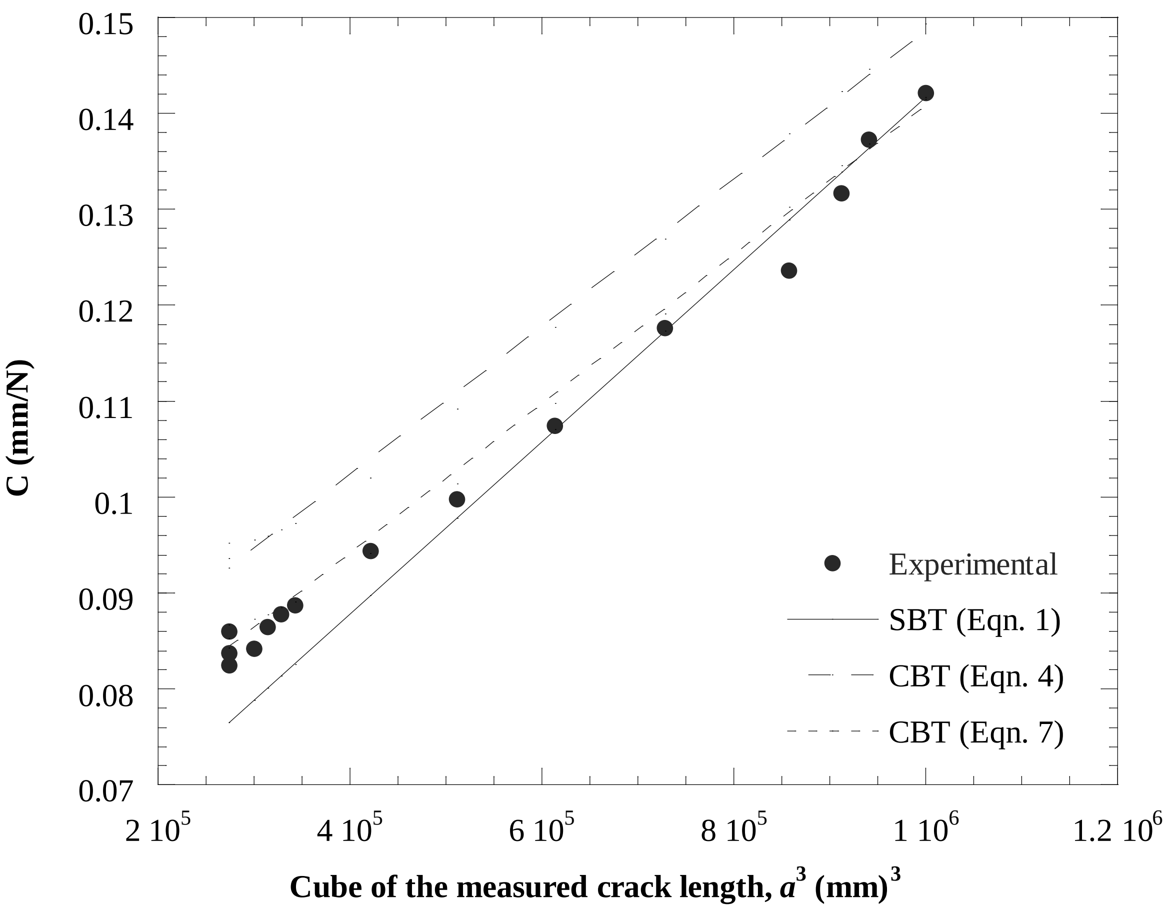

Figure 6. Values of the compliance, C, versus a^3 for a joint bonded with the epoxy-paste adhesive. (Experimental values are the points, and values predicted via equations (1), (4) and (7) are shown as the lines).

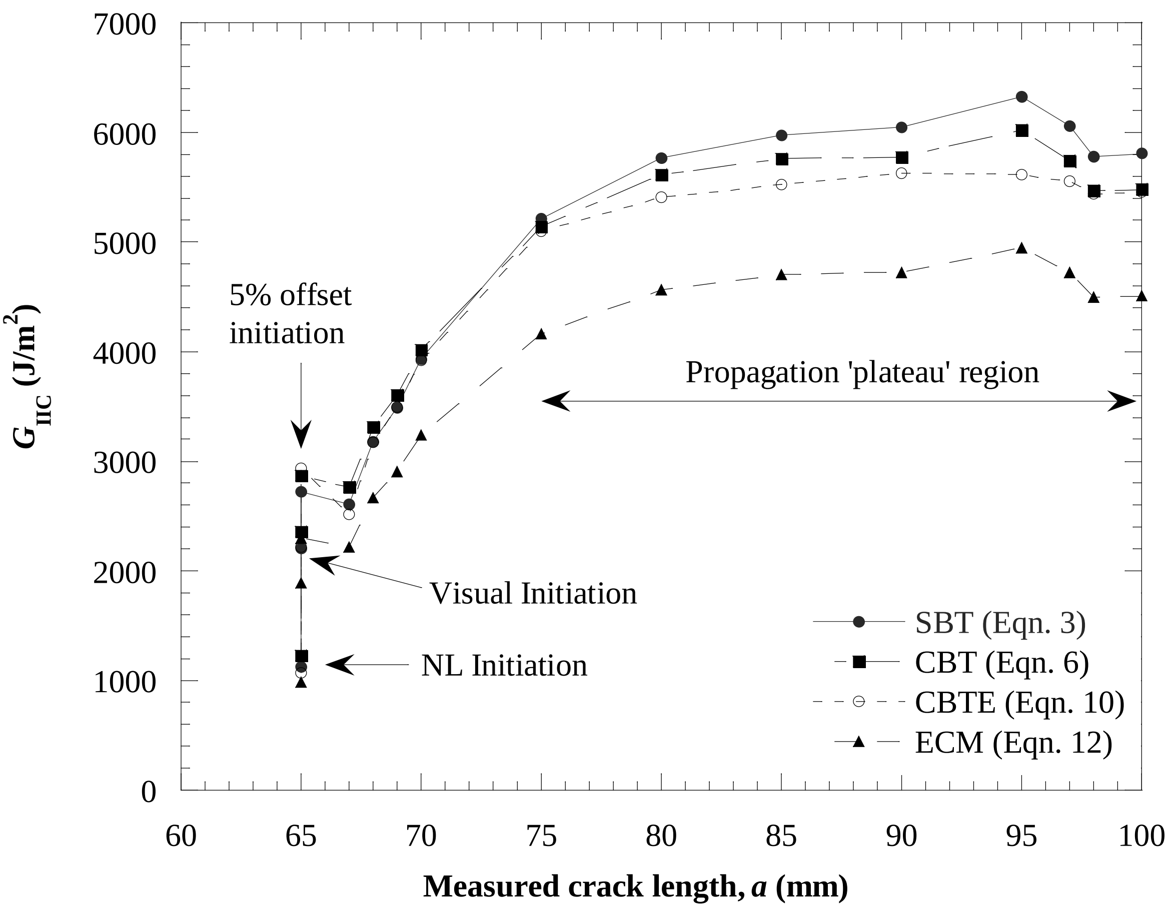

Figure 7. Typical resistance curves (G_{IIC} versus measured crack length) for a joint bonded with the epoxy-paste adhesive. (G_{IIC} values deduced via: Simple Beam Theory, equation (3); Corrected Beam Theory (CBT) equation (6); corrected beam theory with effective crack length (CBTE) equation (10); and Experimental Compliance Method (ECM) equation (12) approaches.)

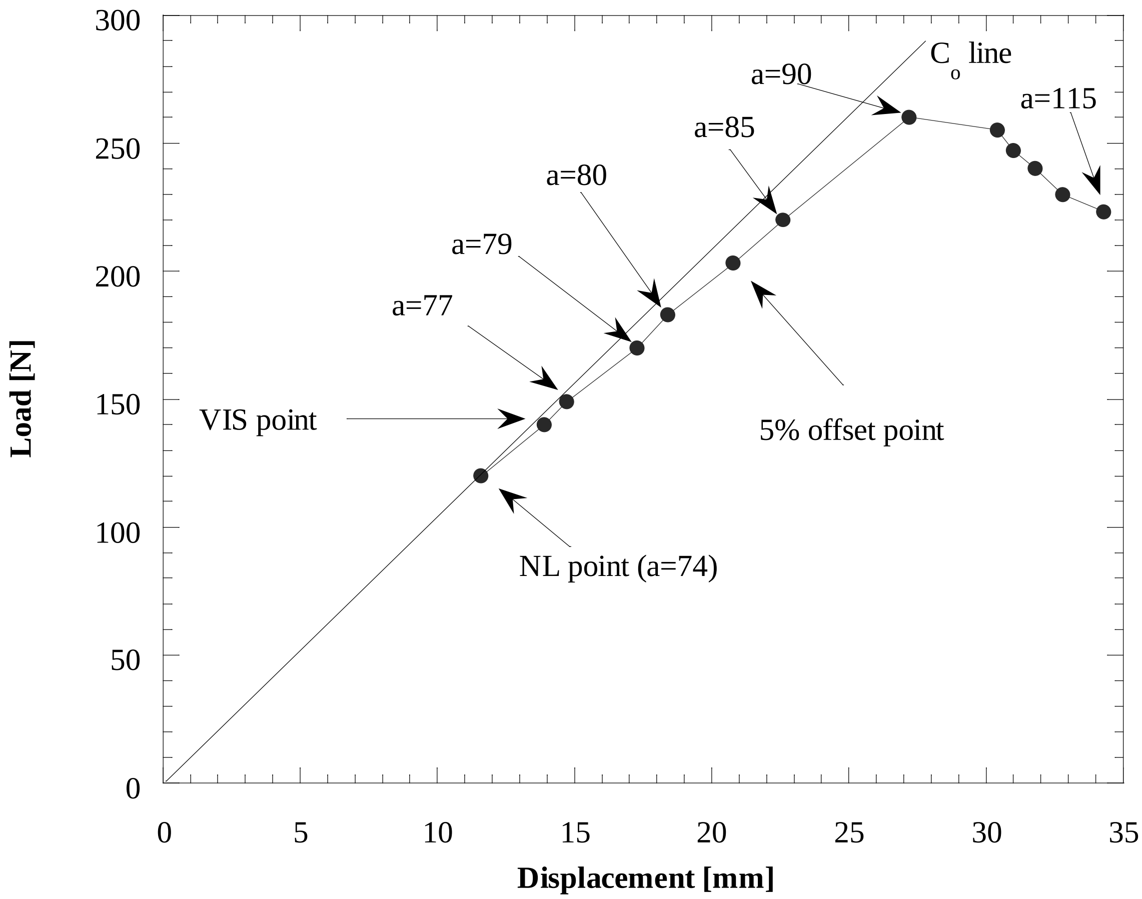

Figure 8. Typical force-displacement trace for a joint bonded with the epoxy-film adhesive. (**Notes: (1) Measured crack length, *a*, values shown are in mm.**).

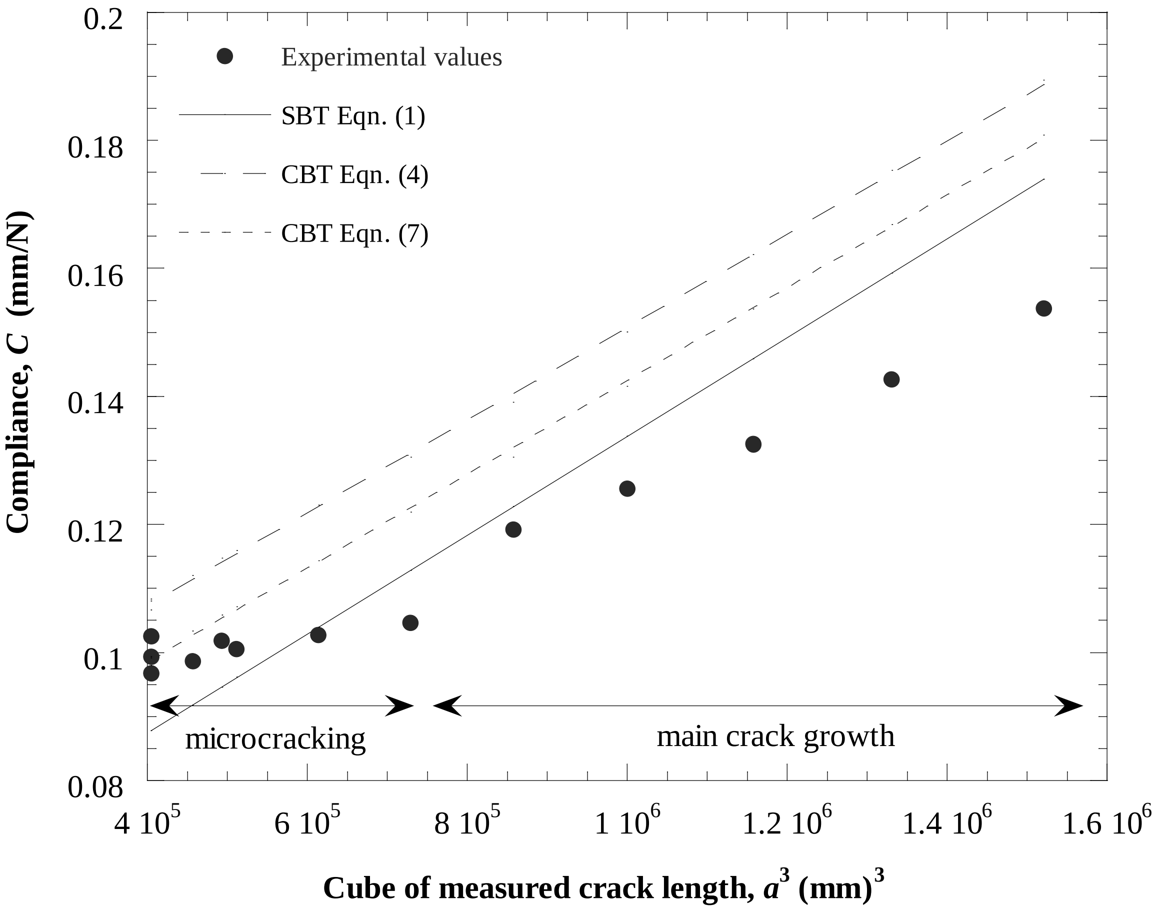

Figure 9. Values of the compliance, C, versus a^3 for a joint bonded with the epoxy-film adhesive.

(a)

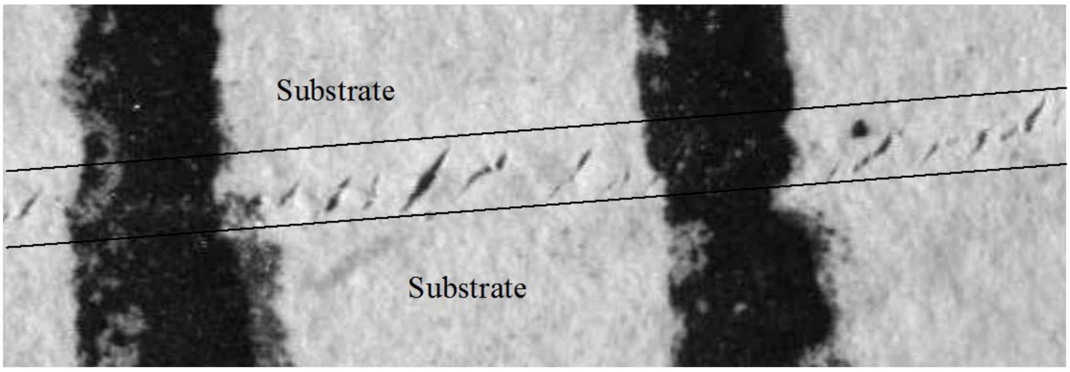

(b)

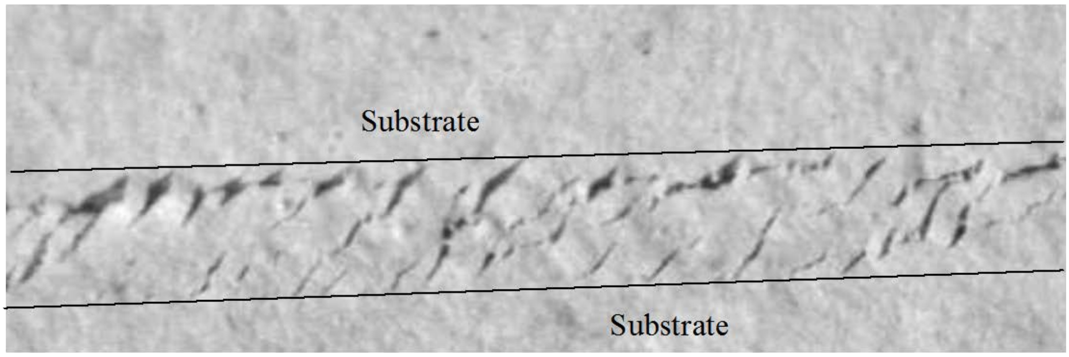

Figure 10. Photographs of microcracking in the adhesive layer for a joint bonded with the epoxy-film adhesive. Magnification: (a) X80 (b) X180. **(Notes: (1) The vertical black lines in (a) are drawn 1mm apart; (2) The direction of crack growth is from left to right).**

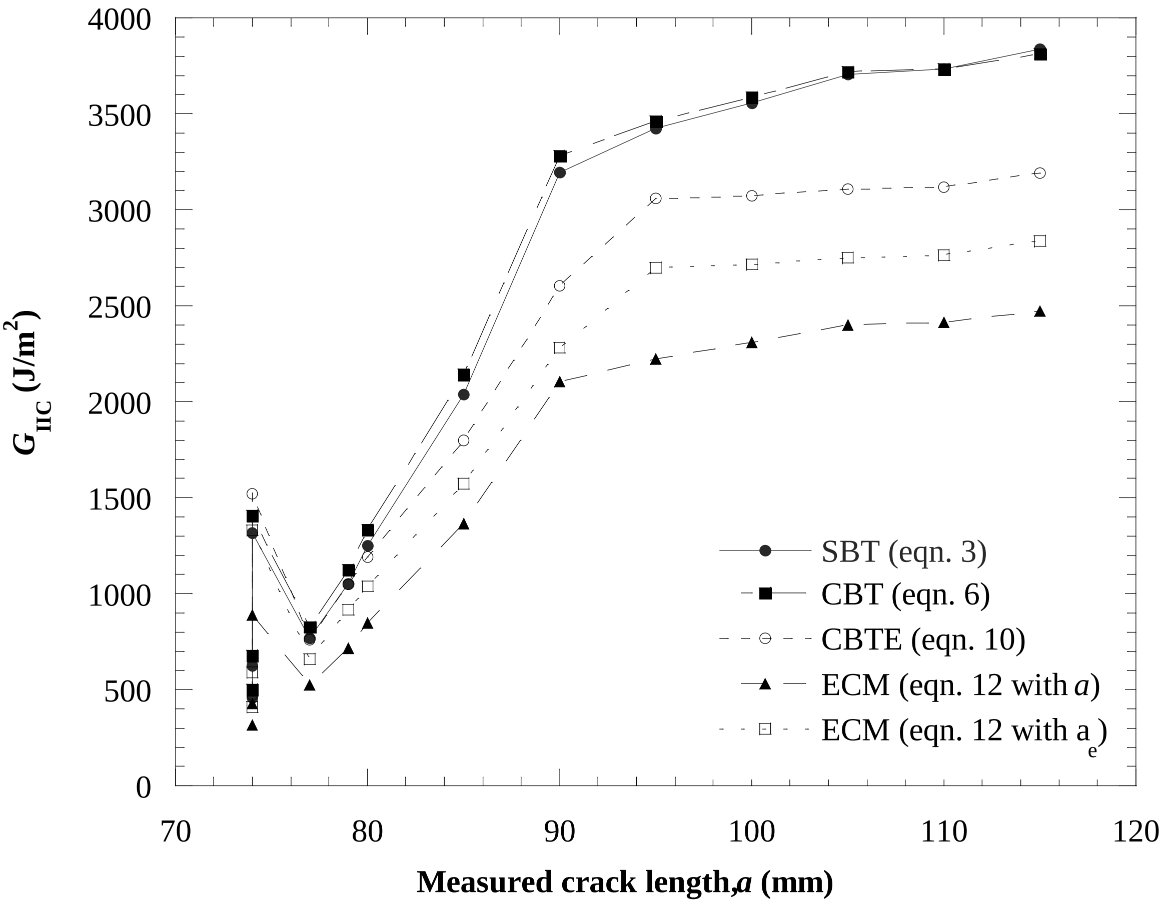

Figure 11. Typical resistance curves (G_{IIC} versus measured crack length) for a joint bonded with the epoxy-film adhesive. (G_{IIC} values deduced via Simple Beam Theory (SBT), Corrected Beam Theory (CBT), Corrected Beam Theory with Effective Crack Length (CBTE), Experimental Compliance Method (ECM with *a*), and Experimental Compliance method with Effective Crack Length approaches.)